European Conference on Optical Communication (ECOC) 2022 © Optica Publishing Group 2022

All-optical Switching using a Photonic Crystal Molecule with Asymmetric Fano Lineshape

Quentin Saudan[(1)*], Dagmawi A. Bekele[(1)], Meng Xiong[(1)], Kresten Yvind[(1)], Jesper Mørk[(1)] and Michael Galili[(1)]

[(1)] Department of Electrical and Photonics Engineering, DTU, *ques@dtu.dk

Abstract *We report 10 Gbps all-optical switching using a photonic molecule based on two lattice-shifted coupled photonic crystal nanocavities in Indium Phosphide. The process is enhanced by the asymmetric Fano resonance lineshape leading to 0.4 dB OSNR penalty at error rates smaller than* 10^{-9} *with switching energies as low as 19.5 fJ/bit or 39 fJ/pulse.*

Introduction

Miniaturization and progress in nano-fabrication have opened the door for the use of photonic crystals in the communication bands [1] and ultra-small cavities with a footprint smaller than 100 $\mu\mathrm{m}^2$. The confinement of the light in such very small volumes contributed to the enhancement of nonlinearities in cavities [2] and enabled low-power all-optical switching [3]. However, these photonic crystal cavities have been extensively studied with a single-mode cavity [3]–[5], where the spectral proximity of the pump with the probe during all-optical switching is such that the optical filtering is challenging and crosstalk is inevitable. This issue was solved by introducing multi-mode cavities [6],[7] or a system of coupled nanocavities called photonic molecule [8],[9]. So far, such coupled resonators have only been studied with Lorentzian lineshapes or at very low repetition rate. We therefore wish to fill this gap by studying the dynamic of a photonic molecule based on an asymmetric Fano resonance when pumped with a high-speed data signal. The advantages of such resonators with respect to standard nanocavities will be discussed, i.e. the total suppression of pump crosstalk leading to minimal added errors at the receiver and a potential gain in overall energy efficiency.

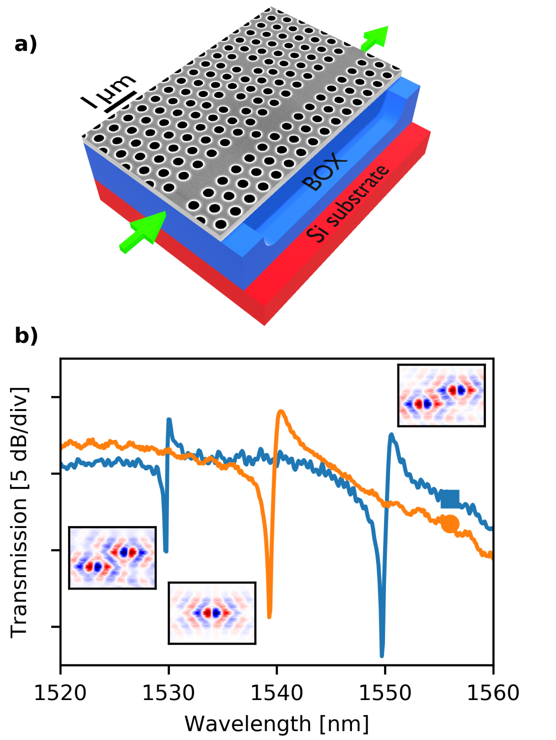

Fig. 1: (a) Illustration of the device structure. The top layer is an SEM image of the photonic crystal molecule side coupled to the waveguide. The lower layers are representations of the $\mathrm{SiO_2}$ buried oxide layer (BOX) and the silicon substrate. **(b)** Measured transmission of the single cavity (orange line) and of the photonic molecule (blue line). The insets show the electric field profile $Re(E_y)$ for the corresponding resonances.

Device

The structure investigated in this paper is based on a photonic crystal membrane using InP-on-insulator platform. The photonic crystal section is membranized to enhance the vertical confinement as illustrated in Fig. 1**(a)**. More details on the fabrication are discussed in Ref. [10].

The photonic molecule is formed by side coupling two lattice-shifted H0 nanocavities, generating two supermodes with a certain resonant wavelength spacing. The photonic molecule is side coupled to a photonic crystal waveguide as shown in the SEM image of Fig. 1**(a)**, leading to asymmetric Fano resonances [11] from the interference between the two available light paths: straight through the waveguide and through the photonic molecule. The parameters for the nanocavities are similar to Ref. [12] with C_1=0.213a, C_2=0.152a and C_3=0.096a, where a=460 nm is the lattice parameter. Compared to the Lorentzian structure reported previously

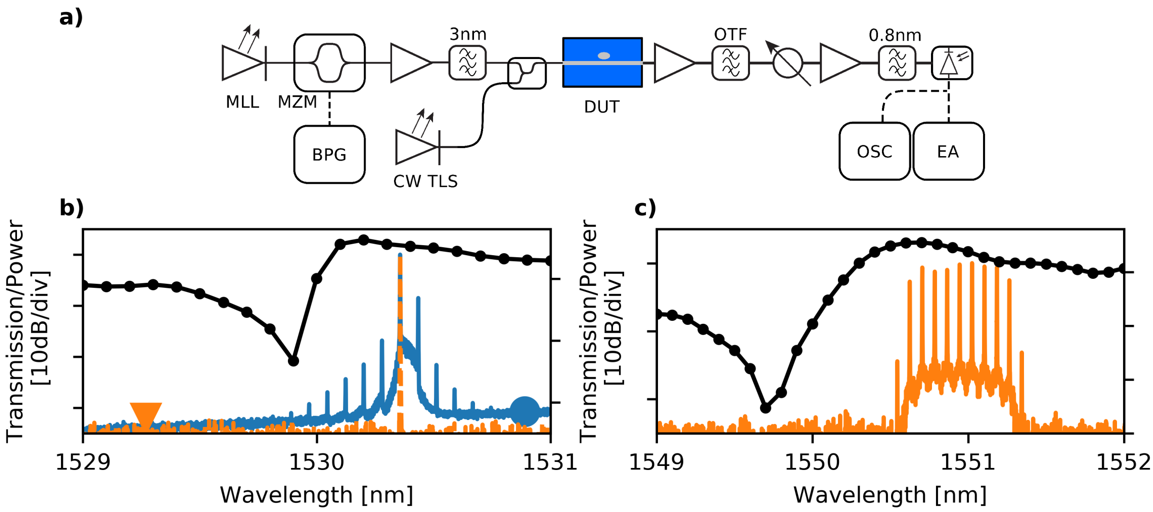

Fig. 2: (a) Schematic of the setup used for wavelength conversion. MLL is mode-locked laser, MZM is Mach-Zehnder modulator, BPG is bit pattern generator, CW TLS is continuous-wave tunable laser source, DUT is device under test, OTF is optical tunable filter, OSC is oscilloscope, EA is error analyser. **(b)** Cold-cavity device transmission (black) and power spectrum of the input (orange/triangle) and output (blue/circle) probe light. **(c)** Cold-cavity device transmission (black) and power spectrum of the input pump light.

[8], the asymmetric Fano resonance has a much smaller peak-to-minimum separation compared to the Lorentzian lineshape with an equivalent quality factor. High-speed signals can therefore be optimally coupled to the resonator system without sacrificing the light confinement and the energy efficiency of the nonlinear process.

The spectra in Fig. 1**(b)** show the transmission of a fabricated device with a photonic molecule in blue and a single H0 cavity in orange. Grating couplers cause the slight skewing of the transmission spectra. The insets correspond to the electric field distribution $Re(E_y)$ extracted from 3D-FDTD simulations for each of the resonances. They confirm the presence of supermodes with opposite parities, leading to the 20 nm wavelength splitting between the resonances. The extinction ratio (ER) as well as the total quality factor (Q_t) of the 1550 nm resonance are close to the standard H0 cavity with ER=31 dB and Q_t=2500. This is not the case for the 1530 nm resonance where we observe a drop of the extinction ratio to ER=16 dB. According to the coupled mode theory, this reflects a higher loaded quality factor Q_L and therefore a higher measured Q_t=5800. The nonlinear mode volume [13] V_{TPA} is roughly doubled from 1.41 $(\lambda/\mathrm{n})^3$ for the H0 cavity to 2.35 $(\lambda/\mathrm{n})^3$ and 2.75 $(\lambda/\mathrm{n})^3$ for the mode at 1550 nm and 1530 nm respectively.

The switching process is accomplished through the strong nonlinearities and light-matter interaction in the photonic crystal nanocavities. In the case of InP, the dominant phenomenon is the two-photon absorption (TPA) leading to free-carrier plasma dispersion [14]. The resulting refractive index change imposes a cavity resonance blueshift, allowing the transmission of a probe light to be controlled by a pump. The use of two modes in this context was also reported with multi-mode cavities [6]. However, there is an inherent limitation to this structure as the overlap integral between the TPA carrier generation, proportional to $|E^4|$, and the effective carrier density in the mode, proportional to $|E^2|$, cannot be maximal with two different modes of a single cavity. In the case of the photonic molecule, the two supermodes only differ by their field symmetry as seen in the insets of 1**(b)** and not by their intensity profile. We therefore observe a nonlinear mode overlap of ≈69%, which is superior to our previous multi-mode cavity investigation [7] and should contribute to reducing the pulse energy for switching.

Wavelength Conversion experiment

The dynamic of the cavity is characterized by performing wavelength conversion of a data signal from a pseudorandom binary sequence (PRBS) 10 Gbps On-Off Keying (OOK) signal onto a continous-wave (CW) probe. As seen in the experimental setup of Fig. 2**(a)**, a train of pulses is generated by a mode-locked laser and gated into a PRBS signal with an intensity modulator. It is then amplified, filtered, combined with the CW probe and injected into the sample via grating couplers with 5 dB insertion loss. The output is preamplified to compensate for the coupling

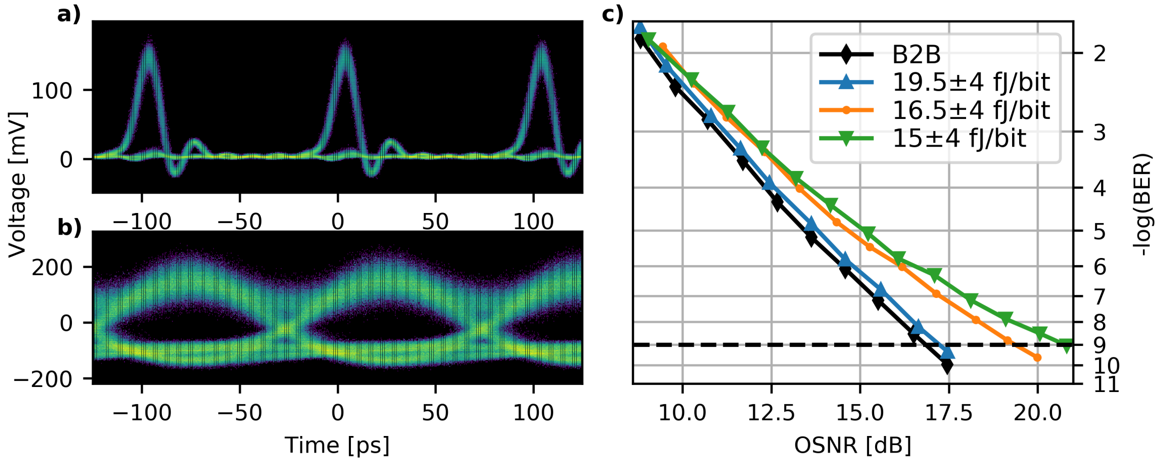

Fig. 3: (a) Eye diagram of the input PRBS signal pump from a 50 GHz DCA scope module. A FWHM of ≈ 12 ps can be observed. **(b)** Eye diagram of the converted signal at error-free (BER $< 10^{-9}$) level with -35.5 dBm received power using a 8 GHz receiver. **(c)** BER curve versus OSNR for the signal pump (B2B) and the converted signal at different pulse energies with error-free OSNR penalties from 0.4 dB to 4 dB.

losses and the pump is completely filtered out by an optical tunable filter. The resulting modulated signal is sent to a 8 GHz receiver and analysed for bit error rate (BER). The fast pulse shape is also recorded by a 50 GHz oscilloscope.

Figures 2**(b)** and **(c)** show the spectral location of the pump and probe compared to the cold resonances of the photonic molecule in the optimal configuration. We chose to couple the pump in the lower Q_t resonance to be able to cast a wider spectrum and therefore a shorter pump pulse, with potentially a drop in energy efficiency due to the lower quality factor. On the other hand, the high Q_t resonance maximizes the impact of the resonance shift on the CW probe light as the transmission slope is much sharper at the resonance. Both pump and probe are blue-detuned with respect to the cold cavity resonance to compensate for the local thermal heating [15] of the cavity during operation.

The 10 Gbps modulated pump injected in the devices has a pulse FWHM of ≈ 12 ps or smaller as shown in the eye diagram of Fig. 3**(a)**. This short pulse signal enhances the nonlinear process in the cavity and lowers the pulse energy compared to a higher duty cycle signal. We achieve an error-free (BER $< 10^{-9}$) modulation of the probe light with a clear eye opening in Fig. 3**(b)** and a minimal OSNR penalty of 0.4 dB compared to the back-to-back BER curve of Fig. 3**(c)** taken at the same wavelength. The energy consumption for the best curve is estimated to be 19.5 fJ/bit or 39 fJ/pulse. This compares well with previously reported values for Lorentzian photonic molecule [8] and single-mode H0 cavities [16]. We also observe a similar impact of the pulse energy on the BER curves : by lowering the pump pulse power and optimizing the probe detuning to the cavity to reduce the impact of thermal resonance shifting, we can still reach error-free operation with an increased OSNR penalty of 4 dB at 15 fJ/bit.

Even though the nonlinear mode volume of the photonic crystal cavity is bigger than the standard single-mode H0 nanocavity, we observe a power consumption smaller than previously reported 10 Gbps wavelength conversion on InP [16] with a smaller power penalty. We attribute this lower consumption to a much better coupling of the pump which compensates for the increase in mode volume. Indeed, in the single-mode case, the pump is usually detuned from the cavity resonance to give space for filtering and therefore the pump is less optimally coupled to the cavity. This issue is completely bypassed with two resonances.

Conclusions

We have successfully fabricated a photonic crystal molecule with an asymmetric Fano lineshape and demonstrated error-free 10 Gbps all-optical switching of such a device at small pulse energies of 39 fJ/pulse with minimal 0.4 dB OSNR penalty. The device has potential to be used for higher modulation speeds in the future and the photonic molecule structure could also be used with other cavity designs.

Acknowledgements

This work was financially supported by ERC Adv. (grant 834410-FANO) and NATEC (grant 86929).

References

[1] N. Moll, S. J. McNab, and Y. A. Vlasov, “Ultra-low loss photonic integrated circuit with membrane-type photonic crystal waveguides”, *Optics Express, Vol. 11, Issue 22, pp. 2927-2939*, vol. 11, no. 22, pp. 2927–2939, Nov. 2003, ISSN: 1094-4087. DOI: 10.1364/OE.11.002927.

[2] A. Shinya, E. Kuramochi, H. Taniyama, *et al.*, “Nonlinear and adiabatic control of high-Q photonic crystal nanocavities”, *Optics Express, Vol. 15, Issue 26, pp. 17458-17481*, vol. 15, no. 26, pp. 17 458–17 481, Dec. 2007, ISSN: 1094-4087. DOI: 10.1364/OE.15.017458.

[3] T. Tanabe, M. Notomi, S. Mitsugi, A. Shinya, and E. Kuramochi, “All-optical switches on a silicon chip realized using photonic crystal nanocavities”, *Applied Physics Letters*, vol. 87, no. 15, p. 151 112, Oct. 2005, ISSN: 0003-6951. DOI: 10.1063/1.2089185.

[4] K. Nozaki, T. Tanabe, A. Shinya, *et al.*, “Sub-femtojoule all-optical switching using a photonic-crystal nanocavity”, *Nature Photonics*, vol. 4, no. 7, pp. 477–483, Jul. 2010. DOI: 10.1038/nphoton.2010.89.

[5] Y. Yu, E. Palushani, M. Heuck, *et al.*, “Switching characteristics of an InP photonic crystal nanocavity: Experiment and theory”, *Optics Express*, vol. 21, no. 25, p. 31 047, Dec. 2013, ISSN: 1094-4087. DOI: 10.1364/oe.21.031047.

[6] K. Nozaki, E. Kuramochi, A. Shinya, and M. Notomi, “25-channel all-optical gate switches realized by integrating silicon photonic crystal nanocavities”, *Optics Express*, vol. 22, no. 12, p. 14 263, Jun. 2014. DOI: 10.1364/OE.22.014263.

[7] Q. Saudan, D. A. Bekele, G. Dong, *et al.*, “Crosstalk-free all-optical switching enabled by Fano resonance in a multi-mode photonic crystal nanocavity”, *Optics Express, Vol. 30, Issue 5, pp. 7457-7466*, vol. 30, no. 5, pp. 7457–7466, Feb. 2022, ISSN: 1094-4087. DOI: 10.1364/OE.449588.

[8] S. Combrié, G. Lehoucq, A. Junay, *et al.*, “All-optical signal processing at 10 GHz using a photonic crystal molecule”, *Applied Physics Letters*, vol. 103, no. 19, p. 193 510, Nov. 2013, ISSN: 0003-6951. DOI: 10.1063/1.4829556.

[9] K. Nozaki, A. Shinya, S. Matsuo, T. Sato, E. Kuramochi, and M. Notomi, “Ultralow-energy and high-contrast all-optical switch involving Fano resonance based on coupled photonic crystal nanocavities”, *Optics Express*, vol. 21, no. 10, p. 11 877, May 2013, ISSN: 1094-4087. DOI: 10.1364/OE.21.011877.

[10] D. A. Bekele, Y. Yu, H. Hu, *et al.*, “Photonic crystal Fano resonances for realizing optical switches, lasers, and non-reciprocal elements”, in *Active Photonic Platforms IX*, International Society for Optics and Photonics, vol. 10345, SPIE, 2017, pp. 107–113. DOI: 10.1117/12.2273801.

[11] S. Fan, “Sharp asymmetric line shapes in side-coupled waveguide-cavity systems”, *Applied Physics Letters*, vol. 80, no. 6, pp. 908–910, 2002, ISSN: 00036951. DOI: 10.1063/1.1448174.

[12] Y. Yu, M. Heuck, H. Hu, *et al.*, “Fano resonance control in a photonic crystal structure and its application to ultrafast switching”, *Applied Physics Letters*, vol. 105, no. 6, p. 061 117, Aug. 2014, ISSN: 0003-6951. DOI: 10.1063/1.4893451.

[13] M. Saldutti, M. Xiong, E. Dimopoulos, Y. Yu, M. Gioannini, and J. Mørk, “Modal Properties of Photonic Crystal Cavities and Applications to Lasers”, *Nanomaterials 2021, Vol. 11, Page 3030*, vol. 11, no. 11, p. 3030, Nov. 2021, ISSN: 2079-4991. DOI: 10.3390/NANO11113030.

[14] B. Bennett, R. Soref, and J. Del Alamo, “Carrier-induced change in refractive index of InP, GaAs and InGaAsP”, *IEEE Journal of Quantum Electronics*, vol. 26, no. 1, pp. 113–122, 1990, ISSN: 00189197. DOI: 10.1109/3.44924.

[15] K. Perrier, S. Greveling, H. Wouters, *et al.*, “Thermo-optical dynamics of a nonlinear gainp photonic crystal nanocavity depend on the optical mode profile”, *OSA Continuum*, vol. 3, no. 7, pp. 1879–1890, Jul. 2020. DOI: 10.1364/OSAC.393842.

[16] Y. Yu, H. Hu, L. K. Oxenløwe, K. Yvind, and J. Mork, “Ultrafast all-optical modulation using a photonic-crystal Fano structure with broken symmetry”, *Optics Letters*, vol. 40, no. 10, p. 2357, May 2015. DOI: 10.1364/OL.40.002357.